



## EFFECT OF ACTIVE MASS IN ELECTRODE DISC ON PERFORMANCE OF $\text{Li}_{1.06}\text{Ni}_{0.313}\text{Co}_{0.313}\text{Mn}_{0.313}\text{O}_2$ CATHODE

Chunxia Gong<sup>1†</sup> --- Guanghua Li<sup>2</sup> --- Lixu Lei<sup>3</sup>

<sup>1</sup>School of Chemistry and Chemical Engineering, Southeast University, Nanjing, China, Zhejiang Tianneng battery (Jiangsu) Co., Ltd., Shuyang Jiangsu, China

<sup>2,3</sup>School of Chemistry and Chemical Engineering, Southeast University, Nanjing, China

### ABSTRACT

$\text{Li}_{1.06}\text{Ni}_{0.313}\text{Co}_{0.313}\text{Mn}_{0.313}\text{O}_2$  sample has been synthesized by calcination of co-precipitated precursors. Scanning electron microscopy shows that sample powders are aggregated microplates with average sizes of 200 nm. Electrochemical tests show that Cell-2.0 which has the least mass in cathode disc presents initially a much higher discharge capacity under a current density of  $135 \text{ mA}\cdot\text{g}^{-1}$ ,  $270 \text{ mA}\cdot\text{g}^{-1}$ ,  $540 \text{ mA}\cdot\text{g}^{-1}$ ,  $810 \text{ mA}\cdot\text{g}^{-1}$ ,  $1080 \text{ mA}\cdot\text{g}^{-1}$  and  $1350 \text{ mA}\cdot\text{g}^{-1}$  than the other cells. And Cell-2.0 exhibits better cycling performance with capacity retention of 95.58 % after 40 cycles at  $270 \text{ mA}\cdot\text{g}^{-1}$  current densities than Cell-2.6(77.18 %), Cell-3.0(74.54 %), Cell-3.2(74.79 %) and Cell-3.6(77.56 %). The cells with a regression equation:  $\text{DC}(\text{mAh}\cdot\text{g}^{-1}) = a \times m(\text{mg}) + b$ , regression coefficient:  $r \geq 0.75216$ ;  $a = 7.16984I(\text{C}) - 61.50523$ , regression coefficient:  $r = 0.95522$ ;  $b = -39.75258I(\text{C}) + 297.48985$ , regression coefficient:  $r = 0.9508$ . Therefore, decreasing the mass in each cathode disc can improve the performance of  $\text{Li}_{1.06}\text{Ni}_{0.313}\text{Co}_{0.313}\text{Mn}_{0.313}\text{O}_2$  cells.

**Keywords:** Electrode materials, Energy storage materials, Oxide materials, Electrochemical reactions, Active mass, Electrode disc.

### Contribution/ Originality

The paper contributes the first example to establishment the regression equation about discharged capacity and the mass in each cathode disc.

## 1. INTRODUCTION

In recent years,  $\text{LiCo}_{1/3}\text{Ni}_{1/3}\text{Mn}_{1/3}\text{O}_2$  has been investigated extensively as an alternative to  $\text{LiCoO}_2$  [1], the currently used cathode material in Li-ion batteries.  $\text{LiCo}_{1/3}\text{Ni}_{1/3}\text{Mn}_{1/3}\text{O}_2$  is isostructural to  $\text{LiCoO}_2$ , in which cobalt, manganese and nickel are trivalent, tetravalent and divalent cations, respectively [2] and can provide higher discharge capacity and better safety characteristics than  $\text{LiCoO}_2$  [3, 4].

Various synthetic methods have been applied to produce  $\text{LiNi}_{1/3}\text{Mn}_{1/3}\text{Co}_{1/3}\text{O}_2$ , such as solid-state method [5], hydrothermal method [6, 7], sol-gel method [8-12], solvent evaporation method [13, 14] and co-precipitation method [15-19]. Among these methods, co-precipitation and sol-gel methods have been found powerful, economic and facile for large scale production [20-22] because the transition-metal ions are precipitated homogeneously and oxidized in the aqueous solution at the molecular level [22].

To improve the performance of  $\text{LiNi}_{1/3}\text{Mn}_{1/3}\text{Co}_{1/3}\text{O}_2$  for high-power consuming electric devices, surface modification has been attempted. For example, the capacity retention can be increased by coating the material with grapheme [23]  $\text{CaF}_2$  [24]  $\text{ZnO}$  [25]  $\text{Cr}_2\text{O}_3$  [26] and LBO glass [27]. The discharging capacity can be raised by coating with  $\text{Cr}_2\text{O}_3$  [26] and LBO glass [27].

Another method to improve the performance of the materials is doping. For example, Al [8], Cu [8], Zr [13], Y [28] and Cr [29] are used to substitute part of Ni, Co or Mn, which can improve the cycle performance of  $\text{LiNi}_{1/3}\text{Co}_{1/3}\text{Mn}_{1/3}\text{O}_2$ . Li-rich layered oxides with composite structures ( $x\text{Li}_2\text{MnO}_3 \cdot (1-x)\text{LiMO}_2$ ,  $\text{M} = \text{Ni, Co, Mn, etc.}$ ) also have been extensively studied as promising cathode materials [30-33]. This paper reports what we have found on the mass in each cathode disc on performance of  $\text{Li}_{1.06}\text{Co}_{0.313}\text{Ni}_{0.313}\text{Mn}_{0.313}\text{O}_2$  cells.

## 2. EXPERIMENTAL

### 2.1. Preparation of the Samples

The precursor was prepared as follows: 10 mmol each of  $\text{Ni}(\text{NO}_3)_2 \cdot 6\text{H}_2\text{O}$ ,  $\text{Mn}(\text{NO}_3)_2 \cdot 6\text{H}_2\text{O}$  and  $\text{Co}(\text{NO}_3)_2 \cdot 6\text{H}_2\text{O}$  were dissolved in 50 ml of deionized water, then an aqueous solution of 60 mmol of  $\text{NaOH}$  was added to the solution under vigorous stirring. After the slurry had been stirred for 12 h at 50 °C in nitrogen atmosphere, it was filtered, washed for three times, and then dried at room-temperature in vacuum.

Sample was prepared by mixing  $\text{LiOH}$  and the precursor in a molar ratio of 1.06:0.94 under grinding in an agate mortar for 20 min at room temperature. The mixture was put into a muffle furnace, and the temperature was raised to 450 °C at a rate of 2 °C/min. After the temperature was maintained for 5 h, the temperature was raised again to 850 °C and kept for 15 h. The final product was collected after the furnace is cooled naturally to room temperature.

## 2.2. Experimental Techniques

X-ray diffraction (XRD) was measured on a SHIMADZU XD-3A using Cu K $\alpha$  radiation,  $\lambda=1.54178\text{\AA}$  and a scanning rate of  $10^\circ/\text{min}$ . The morphology and microstructure of the product was characterized by a scanning electron microscope (SEM, FESEM Hitachi S-4800 II). Chemical composition of the sample was determined using an inductively coupled plasma/atomic emission spectrometer (ICP-MS, PE ELAN-9000). The electrochemical performance of the sample was evaluated with a standard CR2032 coin cell with a lithium disc as the negative electrode, a polypropylene membrane (Celgard 2300) as the separator and 1 M LiPF $_6$  in ethylene carbonate (EC) - dimethyl carbonate (DMC) as the electrolyte. The cathode was prepared by coating a slurry consisting of a sample (80 wt. %), acetylene black (10wt. %), and poly(vinylidene fluoride) (PVDF) (10wt.%) dispersed in 1-methyl-2-pyrrolidinone (NMP) onto an aluminum foil with an agate pestle. The cathode was then dried at 100 °C for 24 h in a vacuum drying oven. The mass in each cathode disc was from 2.0 to 3.6 mg. All cells were assembled in an argon-filled glove box. The cells with the cathode which have the mass of 2.0 mg, 2.6 mg, 3.0 mg, 3.2 mg and 3.6 mg named Cell-2.0, Cell-2.6, Cell-3.0, Cell-3.2 and Cell-3.6, respectively.

The charge and discharge tests were performed in the potential range of 2.0-4.5 V at room temperature on a multichannel battery cycling unit (LAND 5.7). Cyclic voltammetry (CV) was determined by an electrochemical workstation (Corrtest CS350) at a sweep rate of  $0.5\text{ mV}\cdot\text{s}^{-1}$ , the reference and auxiliary electrodes were the lithium disc. The electrochemical impedance spectroscopy (EIS) was also done with the coin cell on electrochemical workstation and a frequency response analyzer controlled by Z-plot. The measurements were performed in the frequency range 100 kHz to 0.001 Hz with AC signal amplitude of 10 mV. Data analysis was done using the software Z view 2.

## 3. RESULTS AND DISCUSSION

### 3.1. Structure and Morphology

The elemental analysis of the sample was performed using ICP technique. As indicated in Table 1, the deduced formula for the sample was  $\text{Li}_{1.06}\text{Ni}_{0.313}\text{Co}_{0.313}\text{Mn}_{0.313}\text{O}_2$ .

**Table-1.** The measured elemental contents of the sample with calculated values in brackets

Li	Ni	Co	Mn
7.39 (7.36)	18.40 (18.39)	18.67 (18.46)	17.84 (17.21)

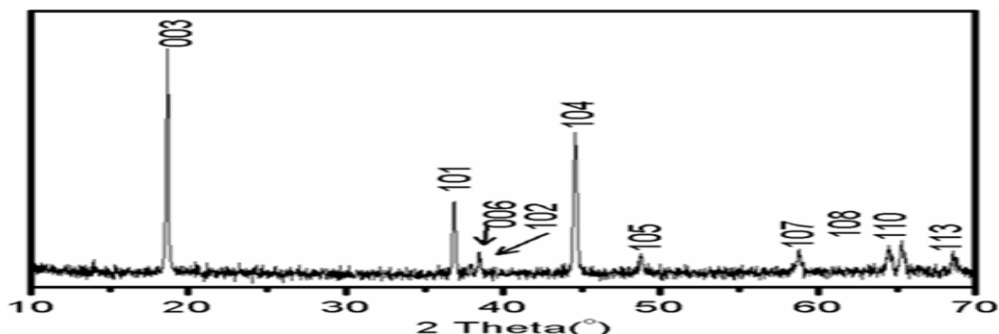


Fig-1. XRD patterns of the sample

Fig. 1 shows the XRD patterns of the sample. For this sample, all the diffraction peaks can be indexed on a hexagonal cell with the space group of  $R\bar{3}m$  as reported [34]. The calculated lattice parameters ( $a$  and  $c$ ), the  $c/a$  values, and the  $I_{(003)}/I_{(104)}$  values are listed in Table 2. It can be seen that the parameters  $a$  and  $c$  are 2.8545 and 14.2218. It is known that cation mixing occurs easily in  $\text{LiCo}_{1/3}\text{Ni}_{1/3}\text{Mn}_{1/3}\text{O}_2$  because the radius of  $\text{Li}^+$  (0.076 nm) is similar to that of  $\text{Ni}^{2+}$  (0.069 nm); and the greater the values of  $I_{(003)}/I_{(104)}$  and  $c/a$ , the better the layered structure develops and the less cation mixing occurs [31]. Here, the values of  $c/a$  (4.9832) and  $I_{(003)}/I_{(104)}$  (1.4048) are a bit higher than  $\text{LiCo}_{1/3}\text{Ni}_{1/3}\text{Mn}_{1/3}\text{O}_2$  (4.9717 and 1.2043), indicating reduces degree of cation mixing in  $\text{Li}_{1.06}\text{Ni}_{0.313}\text{Co}_{0.313}\text{Mn}_{0.313}\text{O}_2$ .

Table-2. Key structural features of the sample

Particle size(nm)	$a(\text{\AA})$	$c(\text{\AA})$	Cell volume ( $\text{\AA}^3$ )	$c/a$	$I_{003}/I_{104}$	Tap density ( $\text{gcm}^{-3}$ )
200	2.8545	14.2218	100.36	4.9832	1.4048	2.1156

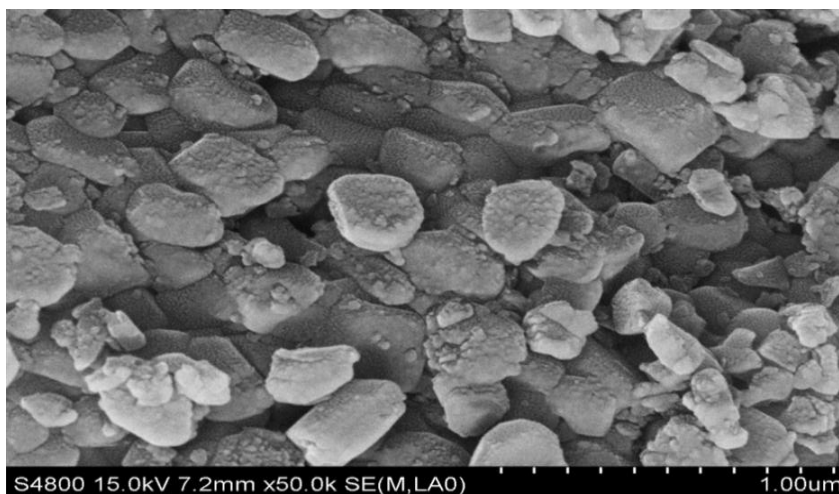


Fig-2. SEM images of the sample

Fig. 2 shows the scanning electron microscopy (SEM) image of the sample, and this sample is microplates with average size of 200 nm. Table 2 also lists the tap densities of the sample, which is  $2.1156 \text{ g cm}^{-3}$ .

### 3.2. Electrochemical Performance

Cyclic voltammetry (CV) was carried out to monitor the electrochemical reactions during charge-discharge process in the voltage range of 2.0–4.5 V at a scan rate of  $0.5 \text{ mVs}^{-1}$ . As shown in Fig. 3 and table 3, Cell-2.0 displays the sharper redox peak and smaller peak potential differences ( $\Delta E$ ) than the other cells. This suggests that faster and better reversibility of the Li intercalation and de-intercalation processes occur on the former electrode [35]. The CV curves of the cells are similar to that of  $\text{LiMn}_{1/3}\text{Co}_{1/3}\text{Ni}_{1/3}\text{O}_2$  in a report.[36]

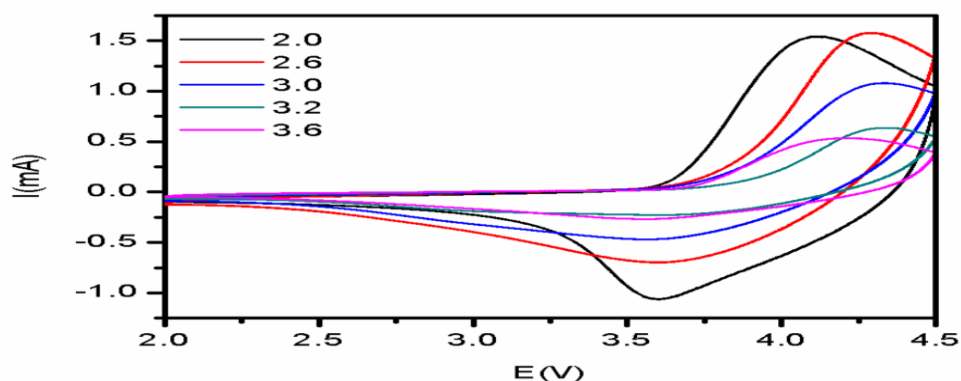


Fig-3. Cyclic voltammetry of the cells

Table-3. Cyclic voltammetry data of the cells

Cells	$E_{p1}$ (V)	$i_{p1}$ (mA)	$E_{p2}$ (V)	$i_{p2}$ (mA)	$\Delta E$ (V)
2.0	4.10839	1.466	3.60622	0.756	0.50217
2.6	4.28844	0.995	3.61126	0.508	0.67718
3.0	4.33294	0.976	3.55934	0.239	0.77360
3.2	4.34202	0.558	3.61214	0.237	0.72988
3.6	4.22327	0.494	3.56782	0.056	0.65535

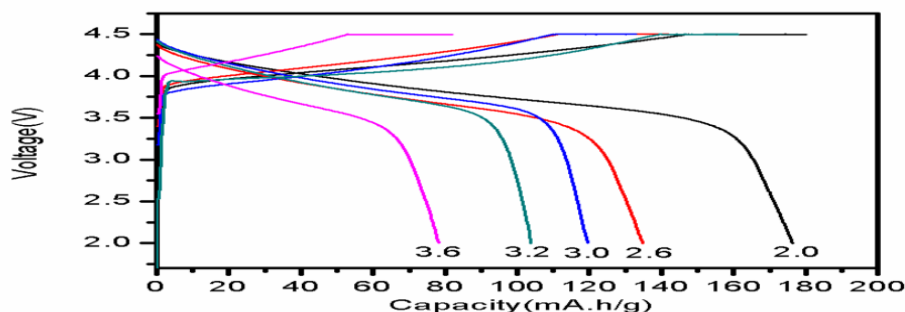


Fig-4. The charge-discharge curves of the cells

Fig. 4 shows the charge-discharge curves of the cells at current densities of  $135\text{mA}\cdot\text{g}^{-1}$ (0.5 C). The initial discharge capacity of Cell-2.0 ( $176.4\text{mAh}\cdot\text{g}^{-1}$ ) is much higher than that of the other cells ( $134.8, 119.7, 103.9$  and  $78.1\text{mAh}\cdot\text{g}^{-1}$ , respectively). This agrees with the CV curves. Fig. 5 shows the curve of discharged capacities at different rates along with cycle number. It can be seen that Cell-2.0 exhibits better cycle performance with capacity retention of 95.58 % after 40 cycles at  $270\text{mA}\cdot\text{g}^{-1}$  current densities than the other cells ( $77.18, 74.54, 74.79$  and  $77.56\%$ ). Therefore, Cell-2.0 brings out better performance.

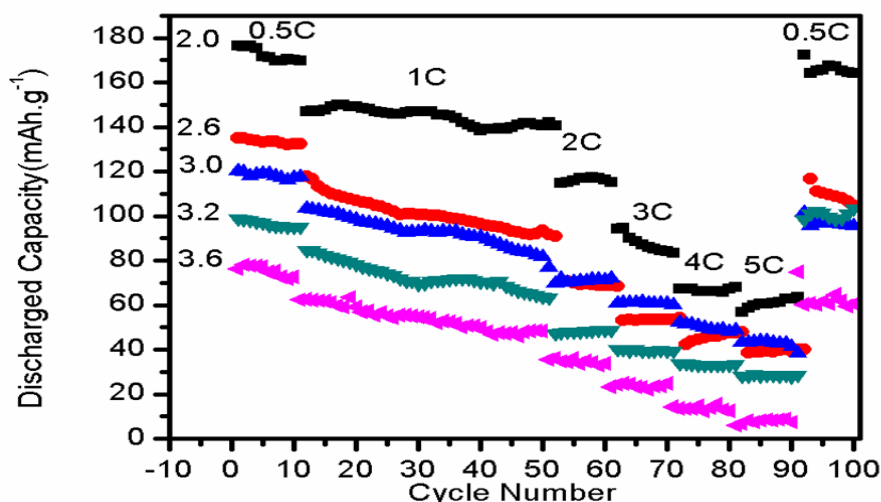


Fig-5. The cycling behavior of the cells

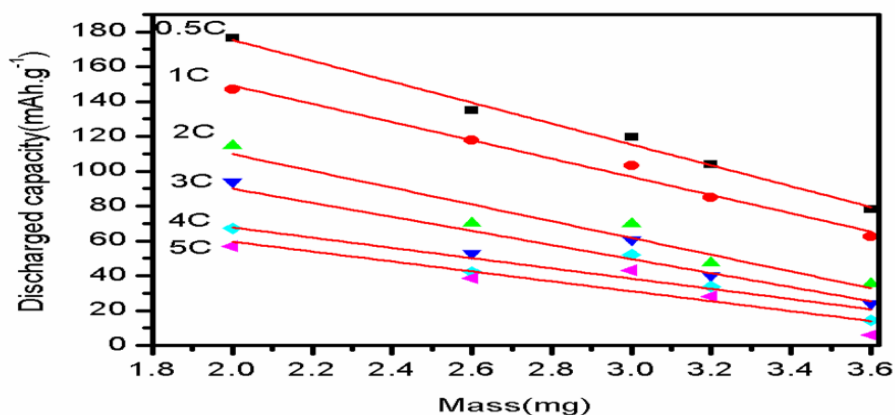


Fig-6. The relation of cathode mass and discharged capacity at different current densities

Fig.6 shows the relation of discharged capacity (DC) and cathode mass (m) at different current densities. At the current densities of  $135\text{mA}\cdot\text{g}^{-1}$ (0.5 C), the cells with a regression equation:  $DC(\text{mAh}\cdot\text{g}^{-1}) = -59.90054m(\text{mg}) + 295.09355$ , regression coefficient:  $r = 0.98945$ ; at the current densities of  $270\text{mA}\cdot\text{g}^{-1}$ (1 C), the cells with a regression equation:  $DC(\text{mAh}\cdot\text{g}^{-1}) = -52.3387m(\text{mg}) + 253.83548$ , regression coefficient:  $r = 0.98133$ ; at the current densities of  $540\text{mA}\cdot\text{g}^{-1}$ (2 C), the cells with a regression equation:  $DC(\text{mAh}\cdot\text{g}^{-1}) = -48.06989m(\text{mg}) + 205.96129$ ,

regression coefficient:  $r = 0.91634$ ; at the current densities of  $810 \text{ mA}\cdot\text{g}^{-1}$  (3 C), the cells with a regression equation:  $DC(\text{mAh}\cdot\text{g}^{-1}) = -40.34946m(\text{mg}) + 170.70645$ , regression coefficient:  $r = 0.85183$ ; at the current densities of  $1080 \text{ mA}\cdot\text{g}^{-1}$  (4 C), the cells with a regression equation:  $DC(\text{mAh}\cdot\text{g}^{-1}) = -29.37097m(\text{mg}) + 126.54839$ , regression coefficient:  $r = 0.75216$  and at the current densities of  $1350 \text{ mA}\cdot\text{g}^{-1}$  (5 C), the cells with a regression equation:  $DC(\text{mAh}\cdot\text{g}^{-1}) = -28.48925m(\text{mg}) + 116.62903$ , regression coefficient:  $r = 0.78085$ .

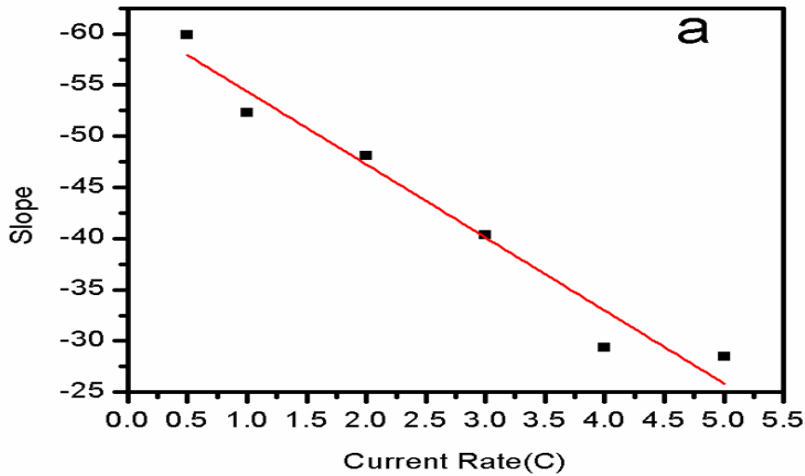


Fig-7a.

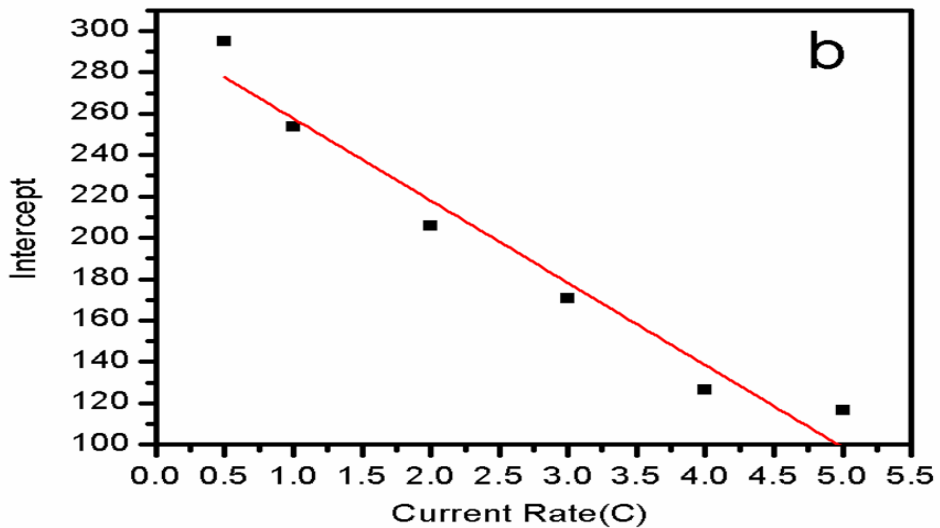


Fig-7b.

Fig-7. The relation of the slope and intercept for cathode mass and discharged capacity line and the current rate

Fig.7a shows the relation of the slope ( $a$ ) for cathode mass and discharged capacity line and the current rate ( $I$ ). The cells with a regression equation:  $a = 7.16984 I(C) - 61.50523$ , regression coefficient:  $r = 0.95522$ ; Fig.7b shows the relation of the intercept ( $b$ ) for cathode mass and discharged capacity line and the current rate ( $I$ ). The cells with a regression equation:  $b = -39.75258 I(C) + 297.48985$ , regression coefficient:  $r = 0.9508$ .

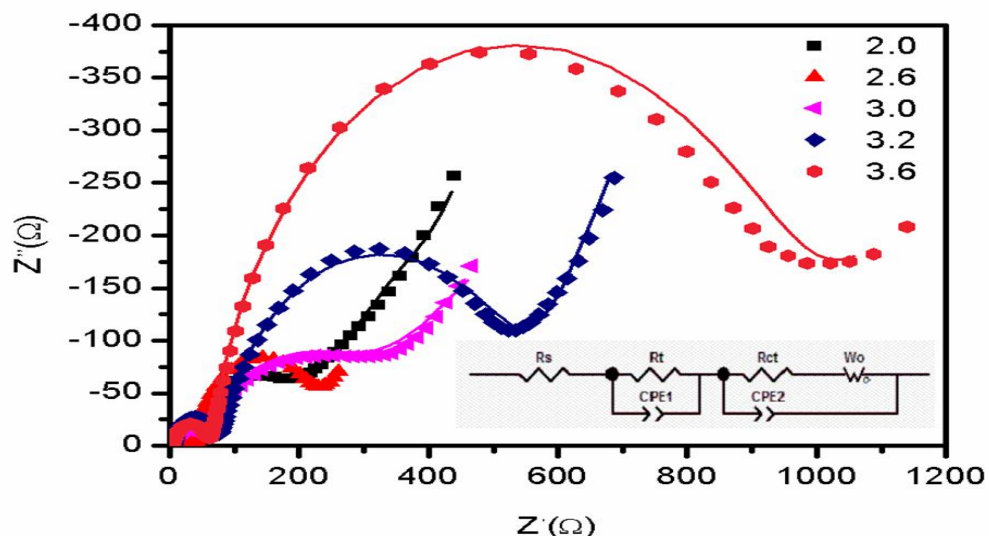


Fig-8. AC impedance spectra of cells in the frequency range from 100 kHz to 0.01 Hz after 2 V discharged.

Table-4. Impedance analysis of the cells

cells	$R_s$	$R_t$	CPE1	$R_{ct}$	CPE2	$W_o$
2.0	5.111	37.78	$6.5017e-5$	158.3	$2.0663e-3$	418.8
2.6	5.501	33.89	$3.8314e-5$	203.6	$3.7601e-3$	182.9
3.0	4.886	50.04	$3.8945e-5$	251.2	$2.2549e-3$	1520
3.2	4.475	71.57	$1.5372e-5$	477.6	$2.2844e-3$	1685
3.6	4.671	58.65	$1.8213e-5$	894.9	$3.3202e-3$	697.2

Fig. 8 shows the Nyquist plots of the cells after 100 charge-discharge cycles between 2 and 4.5 V at the current density of  $135 \text{ mA}\cdot\text{g}^{-1}$ , Table 4 lists the parameters for the simulated circuit. It is clear that the charge-transfer resistances of Cell-2.0 are smaller than the other cells, which again shows that decrease the mass in each cathode disc can improve the performance of  $\text{Li}_{1.06}\text{Ni}_{0.313}\text{Co}_{0.313}\text{Mn}_{0.313}\text{O}_2$  cells.

#### 4. CONCLUSIONS

Sample of a ternary Li-ion battery cathode material  $\text{Li}_{1.06}\text{Ni}_{0.313}\text{Co}_{0.313}\text{Mn}_{0.313}\text{O}_2$  has been successfully synthesized by baking a co-precipitated precursor,  $\text{NiCoMn}(\text{OH})_6$  with LiOH. The sample is aggregated microplates. The cells with a regression equation:  $DC(\text{mAh}\cdot\text{g}^{-1})=a\times m(\text{mg})+b$ , regression coefficient:  $r \geq 0.75216$ ;  $a = 7.16984I(C) - 61.50523$ , regression coefficient:  $r = 0.95522$ ;  $b = -39.75258I(C) + 297.48985$ , regression coefficient:  $r = 0.9508$ . Decrease the mass in each disc can improve the performance of  $\text{Li}_{1.06}\text{Ni}_{0.313}\text{Co}_{0.313}\text{Mn}_{0.313}\text{O}_2$  cell.

#### 5. ACKNOWLEDGEMENTS

We would like to thank The Office of Personnel, Jiangsu Province and The Southeast University for financial supports.

## REFERENCES

- [1] X. J. Wang, Q. T. Qu, Y. Y. Hou, F. X. Wang, and Y. P. Wu, "An aqueous rechargeable lithium battery of high energy density based on coated Li metal and  $\text{LiCoO}_2$ ," *Chemical Communications*, vol. 49, pp. 6179-6181, 2013.
- [2] T. Ohzuku and Y. Makimura, "Layered lithium insertion material of  $\text{LiCo}_{1/3}\text{Ni}_{1/3}\text{Mn}_{1/3}\text{O}_2$  for lithium-ion batteries," *Chemistry Letters*, vol. 7, pp. 642-643, 2001.
- [3] K. M. Shaju, G. V. S. Rao, and B. V. R. Chowdari, "Performance of layered  $\text{Li}(\text{Ni}_{1/3}\text{Co}_{1/3}\text{Mn}_{1/3})\text{O}_2$  as cathode for Li-ion batteries," *Electrochimica Acta*, vol. 48, pp. 145-151, 2002.
- [4] Y. Koyama, I. Tanaka, H. Adachi, Y. Makimura, and T. Ohzuku, "Crystal and electronic structures of superstructural  $\text{Li}_{1-x}\text{Co}_{1/3}\text{Ni}_{1/3}\text{Mn}_{1/3}\text{O}_2$  ( $0 \leq x \leq 1$ )," *Journal of Power Sources*, vol. 119, pp. 644-648, 2003.
- [5] L. Tan and H. W. Liu, "High rate charge-discharge properties of  $\text{LiNi}_{1/3}\text{Co}_{1/3}\text{Mn}_{1/3}\text{O}_2$  synthesized via a low temperature solid-state method," *Solid State Ionics*, vol. 181, pp. 1530-1533, 2010.
- [6] J. L. Xie, X. A. Huang, Z. B. Zhu, and J. H. Dai, "Hydrothermal synthesis of  $\text{Li}(\text{Ni}_{1/3}\text{Co}_{1/3}\text{Mn}_{1/3})\text{O}_2$  for lithium rechargeable batteries," *Ceramics International*, vol. 36, pp. 2485-2487, 2010.
- [7] Y. F. Su, F. Wu, M. Wang, L. Y. Bao, and S. Chen, "A novel method for synthesis of layered  $\text{LiNi}_{1/3}\text{Mn}_{1/3}\text{Co}_{1/3}\text{O}_2$  as cathode material for lithium-ion battery," *Journal of Power Sources*, vol. 195, pp. 2362-2367, 2010.
- [8] J. Molenda, A. Milewska, and M. Molenda, "Structural, transport and electrochemical properties of  $\text{LiNi}_{1-y}\text{Co}_y\text{Mn}_{0.1}\text{O}_2$  and Al, Mg and Cu-substituted  $\text{LiNi}_{0.65}\text{Co}_{0.25}\text{Mn}_{0.1}\text{O}_2$  oxides," *Solid State Ionics*, vol. 192, pp. 313-320, 2011.
- [9] Y. K. Zhou, Y. Y. Hu, J. Wang, and Z. P. Shao, "Preparation and characterization of macroporous  $\text{LiNi}_{1/3}\text{Co}_{1/3}\text{Mn}_{1/3}\text{O}_2$  using carbon sphere as template," *Materials Chemistry and Physics*, vol. 129, pp. 296-300, 2011.
- [10] Z. D. Huang, X. M. Liu, S. W. Oh, B. A. Zhang, P. C. Ma, and J. K. Kim, "Microscopically porous, interconnected single crystal  $\text{LiNi}_{1/3}\text{Co}_{1/3}\text{Mn}_{1/3}\text{O}_2$  cathode material for Lithium ion batteries," *Journal of Materials Chemistry*, vol. 21, pp. 10777-10784, 2011.
- [11] Z. D. Huang, X. M. Liu, B. A. Zhang, S. W. Oh, P. C. Ma, and J. K. Kim, " $\text{LiNi}_{1/3}\text{Co}_{1/3}\text{Mn}_{1/3}\text{O}_2$  with a novel one-dimensional porous structure: A high-power cathode material for rechargeable Li-ion batteries," *Scripta Materialia*, vol. 64, pp. 122-125, 2011.
- [12] Y. Y. Hu, Y. K. Zhou, J. Wang, and Z. P. Shao, "Preparation and characterization of macroporous  $\text{LiNi}_{1/3}\text{Co}_{1/3}\text{Mn}_{1/3}\text{O}_2$  using carbon sphere as template," *Materials Chemistry and Physics*, vol. 129, pp. 296-300, 2011.
- [13] H. B. Ren, X. Y. Liu, H. P. Zhao, Z. H. Peng, and Y. H. Zhou, "Electrochemical properties of submicron-sized  $\text{LiNi}_{1/3}\text{Co}_{1/3}\text{Mn}_{1/3}\text{O}_2$  cathode materials for lithium-ion battery," *International Journal of Electrochemical Science*, vol. 6, pp. 727-738, 2011.
- [14] H. B. Ren, X. Lie, and Z. H. Peng, "Electrochemical properties of  $\text{LiNi}_{1/3}\text{Mn}_{1/3}\text{Al}_{1/3-x}\text{Co}_x\text{O}_2$  as a cathode material for lithium ion battery," *Electrochimica Acta*, vol. 56, pp. 7088-7091, 2011.

- [15] H. W. Liu and L. Tan, "High rate performance of novel cathode material  $\text{Li}_{1.33}\text{Ni}_{1/3}\text{Co}_{1/3}\text{Mn}_{1/3}\text{O}_2$  for lithium ion batteries," *Materials Chemistry and Physics*, vol. 129, pp. 729-732, 2011.
- [16] Y. S. Lee, K. S. Lee, Y. K. Sun, Y. M. Lee, and D. W. Kim, "Effect of an organic additive on the cycling performance and thermal stability of lithium-ion cells assembled with carbon anode and  $\text{LiNi}_{1/3}\text{Co}_{1/3}\text{Mn}_{1/3}\text{O}_2$  cathode," *Journal of Power Sources*, vol. 196, pp. 6997-7001, 2011.
- [17] T. E. Hong, E. D. Jeong, S. R. Baek, M. R. Byeon, Y. S. Lee, F. N. Khan, and H. S. Yang, "Nano SIMS characterization of boron and aluminum-coated  $\text{LiNi}_{1/3}\text{Co}_{1/3}\text{Mn}_{1/3}\text{O}_2$  cathode materials for lithium secondary ion batteries," *Journal of Applied Electrochemistry*, vol. 42, pp. 41-46, 2012.
- [18] P. X. Zhang, L. Zhang, X. Z. Ren, Q. H. Yuan, J. H. Liu, and Q. L. Zhang, "Preparation and electrochemical properties of  $\text{LiNi}_{1/3}\text{Co}_{1/3}\text{Mn}_{1/3}\text{O}_2$ -PPy composites cathode materials for lithium-ion battery," *Synthetic Metals*, vol. 161, pp. 1092-1097, 2011.
- [19] C. X. Ding, Y. C. Bai, X. Y. Feng, and C. H. Chen, "Improvement of electrochemical properties of layered  $\text{LiNi}_{1/3}\text{Co}_{1/3}\text{Mn}_{1/3}\text{O}_2$  positive electrode material by zirconium doping," *Solid State Ionics*, vol. 189, pp. 69-73, 2011.
- [20] R. Santhanam and B. Rambabu, "High rate cycling performance of  $\text{Li}_{1.05}\text{Ni}_{1/3}\text{Co}_{1/3}\text{Mn}_{1/3}\text{O}_2$  materials prepared by sol-gel and co-precipitation methods for lithium-ion batteries," *Journal of Power Sources*, vol. 195, pp. 4313-4317, 2010.
- [21] F. Wu, M. Wang, Y. F. Su, L. Y. Bao, and S. Chen, "A novel method for synthesis of layered  $\text{LiNi}_{1/3}\text{Mn}_{1/3}\text{Co}_{1/3}\text{O}_2$  as cathode material for lithium-ion battery," *Journal of Power Sources*, vol. 195, pp. 2362-2367, 2010.
- [22] A. M. A. Hashem, A. E. Abdel-Ghany, A. E. Eid, J. Trottier, K. Zaghbi, A. Mauger, and C. M. Julien, "Study of the surface modification of  $\text{LiNi}_{1/3}\text{Co}_{1/3}\text{Mn}_{1/3}\text{O}_2$  cathode material for lithium ion battery," *Journal of Power Sources*, vol. 196, pp. 8632-8637, 2011.
- [23] C. V. Rao, A. L. M. Reddy, Y. Ishikawa, and P. M. Ajayan, " $\text{LiNi}_{1/3}\text{Co}_{1/3}\text{Mn}_{1/3}\text{O}_2$ -Graphene composite as a promising cathode for lithium-ion batteries," *Acs Applied Materials & Interfaces*, vol. 3, pp. 2966-2972, 2011.
- [24] K. Xu, Z. Jie, R. Li, Z. Chen, S. Wu, J. Gu, and J. Chen, "Synthesis and electrochemical properties of  $\text{CaF}_2$ -coated for long-cycling  $\text{Li}[\text{Mn}_{1/3}\text{Co}_{1/3}\text{Ni}_{1/3}]\text{O}_2$  cathode materials," *Electrochimica Acta*, vol. 60, pp. 130-133, 2012.
- [25] L. Tan and H. W. Liu, "Influence of ZnO coating on the structure, morphology and electrochemical performances for  $\text{LiNi}_{1/3}\text{Co}_{1/3}\text{Mn}_{1/3}\text{O}_2$  material," *Russian Journal of Electrochemistry*, vol. 47, pp. 156-160, 2011.
- [26] X. W. Li, Y. B. Lin, Y. Lin, H. Lai, and Z. G. Huang, "Surface modification of  $\text{LiNi}_{1/3}\text{Co}_{1/3}\text{Mn}_{1/3}\text{O}_2$  with  $\text{Cr}_2\text{O}_3$  for lithium ion batteries," *Rare Metals*, vol. 31, pp. 140-144, 2012.
- [27] J. Q. Dou, X. Y. Kang, T. Wumaier, H. W. Yu, N. Hua, Y. Han, and G. Q. Xu, "Effect of lithium boron oxide glass coating on the electrochemical performance of  $\text{LiNi}_{1/3}\text{Co}_{1/3}\text{Mn}_{1/3}\text{O}_2$ ," *Journal of Solid State Electrochemistry*, vol. 16, pp. 1481-1486, 2012.

- [28] Y. W. Li, Y. X. Li, S. K. Zhong, F. P. Li, and J. W. Yang, "Synthesis and electrochemical properties of Y-doped  $\text{LiNi}_{1/3}\text{Mn}_{1/3}\text{Co}_{1/3}\text{O}_2$  cathode materials for Li-Ion battery," *Integrated Ferroelectrics*, vol. 127, pp. 150-156, 2011.
- [29] M. H. Jaafar, N. S. Mohamed, R. Yahya, and N. Kamarulzaman, "LiMn<sub>0.5</sub>Co<sub>0.3</sub>Ni<sub>0.3</sub>Cr<sub>0.1</sub>O<sub>2</sub> cathode materials prepared via sol-gel and combustion methods," *International Congress on Advances in Applied Physics and Materials Science*, vol. 1400, pp. 280-285, 2011.
- [30] J.M. Zheng, D.R. Zhu, Y. Yang, and Y.S. Fung, "The effects of N-methyl-N-butylpyrrolidinium bis(trifluoromethylsulfonyl)imide-based electrolyte on the electrochemical performance of high capacity cathode material  $\text{Li}[\text{Li}_{0.2}\text{Mn}_{0.54}\text{Ni}_{0.13}\text{Co}_{0.13}]\text{O}_2$ ," *Electrochimica Acta*, vol. 59, pp. 14-22, 2012.
- [31] X.H. Zhang, C. Yu, X.D. Huang, J. Zheng, X.F. Guan, D. Luo, and L.P. Li, "Novel composites  $\text{Li}[\text{Li}_x\text{Ni}_{0.34-x}\text{Mn}_{0.47}\text{Co}_{0.19}]\text{O}_2$  ( $0.18 \leq x \leq 0.21$ ): Synthesis and application as high-voltage cathode with improved electrochemical performance for lithium ion batteries," *Electrochimica Acta*, vol. 81, pp. 233-238, 2012.
- [32] J. Wang, M.H. Zhang, C.L. Tang, Y.G. Xia, and Z. P. Liu, "Microwave-irradiation synthesis of  $\text{Li}_{1.3}\text{Ni}_x\text{Co}_y\text{Mn}_{1-x-y}\text{O}_{2.4}$  cathode materials for lithium ion batteries," *Electrochimica Acta*, vol. 80, pp. 15-21, 2012.
- [33] J. Wang, G.X. Yuan, M.H. Zhang, B. Qiu, Y.G. Xia, and Z.P. Liu, "The structure, morphology, and electrochemical properties of  $\text{Li}_{1+x}\text{Ni}_{1/6}\text{Co}_{1/6}\text{Mn}_{4/6}\text{O}_{2.25+x/2}$  ( $0.1 \leq x \leq 0.7$ ) cathode materials," *Electrochimica Acta*, vol. 66, pp. 61-66, 2012.
- [34] J. W. Lee, J. H. Lee, T. T. Viet, J. Y. Lee, J. S. Kim, and C. H. Lee, "Synthesis of  $\text{LiNi}_{1/3}\text{Co}_{1/3}\text{Mn}_{1/3}\text{O}_2$  cathode materials by using a supercritical water method in a batch reactor," *Electrochimica Acta*, vol. 55, pp. 3015-3021, 2010.
- [35] S. Y. Yang, X. Y. Wang, Q. Q. Chen, X. K. Yang, J. J. Li, and Q. L. Wei, "Effects of complexants on  $\text{Ni}_{1/3}\text{Co}_{1/3}\text{Mn}_{1/3}\text{CO}_3$  morphology and electrochemical performance of  $\text{LiNi}_{1/3}\text{Co}_{1/3}\text{Mn}_{1/3}\text{O}_2$ ," *Journal of Solid State Electrochemistry*, vol. 16, pp. 481-490, 2012.
- [36] P. Gao, G. Yang, H. D. Liu, L. Wang, and H. S. Zhou, "Lithium diffusion behavior and improved high rate capacity of  $\text{LiNi}_{1/3}\text{Co}_{1/3}\text{Mn}_{1/3}\text{O}_2$  as cathode material for lithium batteries," *Solid State Ionics*, vol. 207, pp. 50-56, 2012.

Views and opinions expressed in this article are the views and opinions of the author(s), Asian Journal of Energy Transformation and Conservation shall not be responsible or answerable for any loss, damage or liability etc. caused in relation to/arising out of the use of the content.